processes

MDPI

Article

Research on Temperature Sensing Method for Three-Core Cable Intermediate Joint Considering Three-Phase Load Imbalance

Xinhai Li [1], Zhifang Zhang [1], Ting Yang [1], Jiangjun Ruan [2,*] and Borui Niu [2]

[1] Guangdong Zhongshan Power Supply Bureau of China Southern Power Grid Co., Ltd., Zhongshan 528401, China; kartter_ssu@163.com (X.L.); zszhangzf@163.com (Z.Z.); yangt0201@126.com (T.Y.)
[2] School of Electrical Engineering and Automation, Wuhan University, Wuhan 430072, China; boruiniu@163.com
* Correspondence: ruan308@126.com

Abstract: Temperature is a key factor affecting the insulation performance and operation safety of cable joints. Accurate acquisition of hot spot temperatures of cable joints is a difficult issue in cable operation and maintenance. Three-core cables may have unbalanced three-phase loads in actual operation. This paper takes a 10 kV three-core cable joint as the research object; based on the temperature field numerical simulation method, it analyzes the diffusion path of the main heat flow inside the joint and establishes an inversion model that fits the hot spot temperature of the joint through the surface temperature of the cable body. At the same time, considering the special situation of the unbalanced three-phase load of a three-core cable, the joint hot spot temperature inversion model of a three-core cable under an unbalanced three-phase load is further established. This paper further uses the cable joint multi-step unbalanced load temperature rise test to verify the accuracy of the cable joint hot spot temperature inversion model. The maximum error of the transient hot spot temperature inversion does not exceed 4.5 °C, and the steady-state error is within 3 °C. A higher inversion accuracy was achieved. The research results of this article can provide a reference for real-time monitoring of the hot spot temperature of cable joints.

Keywords: cable joints; finite element simulation; hot spot temperature inversion; three-phase unbalance; fault monitoring

Citation: Li, X.; Zhang, Z.; Yang, T.; Ruan, J.; Niu, B. Research on Temperature Sensing Method for Three-Core Cable Intermediate Joint Considering Three-Phase Load Imbalance. *Processes* **2024**, *12*, 496. https://doi.org/10.3390/pr12030496

Academic Editor: Wen-Jer Chang

Received: 30 January 2024
Revised: 22 February 2024
Accepted: 24 February 2024
Published: 28 February 2024

1. Introduction

The operation status and health status of power cables are directly related to the safe and stable operation of the distribution network [1,2]. Cable joints are the weakest link in cable insulation, and their faults have always been high in the proportion of cable faults. Temperature is one of the decisive factors affecting the insulation performance and service life of cable joints [3]. Due to the thicker insulation layer and the presence of contact resistance, the conductor temperature of cable joints is often much higher than that of the cable body, which is the bottleneck point of cable thermal aging. The perception and calculation of cable joint temperature is of great significance for ensuring the power supply reliability of cable lines [4,5].

At present, the methods for calculating the hot spot temperature of cable joints can be divided into thermal path modeling method, numerical calculation method, data mining method, and direct temperature measurement method. The thermal path model method and numerical calculation method can achieve a more accurate calculation of cable joint temperature, which is based on the accurate grasp of cable joint structure and material thermal property parameters. Huang Jingjing [6] and Jiang Heqi [7] and others fully considered the influence of soil, environmental moisture, and adjacent cables when constructing a cable thermal path model, established an equivalent thermal path model of the surrounding environment, and achieved high accuracy. Bian Xiaoyan [8] constructed an RC trapezoidal thermal network model for submarine cables and surrounding soil using a

layered modeling approach and verified the effectiveness of the model using finite element calculation methods. Liang Yongchun [9] established an equivalent two-branch transient thermal circuit model for complex cable structures and heat dissipation environments and short-term and long-term transient thermal circuit models for directly buried cables. YANG F [10,11] established an electromagnetic thermal coupling calculation model for cable joints based on the three-dimensional finite element method. The power loss of the cable was calculated using the electromagnetic field and then loaded into the temperature field for analysis. Zhang Xipeng et al. [12] constructed a three-dimensional simulation model of 10 kV XLPE cable joints and conducted an electromagnetic thermal coupling simulation using finite element calculation methods.

In the case of unclear cable joint structure and material parameters, the hot spot temperature of the joint can also be obtained through data mining and direct measurement. Xiao Wei [13] used the temperature of the left cable sheath, the temperature of the right cable sheath, the temperature of the left cable skin, the temperature of the right cable skin, the ambient temperature, and the cable current as input variables and the temperature of the joint conductor as an output variable. He used a generalized regression neural network to predict the temperature of the cable joint. Wu Tian [14] used cable surface temperature and current data as input variables and used an improved sparrow search algorithm and BP neural network to predict cable core temperature. Yuan Yanling [15] used the support vector machine method to predict the hot spot temperature of cable joints based on their surface temperature. During cable manufacturing, Lv Gengmin [16] preinstalled temperature-measuring optical fibers inside the cable dividing conductor. The preinstalled optical fibers inside the cable dividing conductor were led out to the outside of the terminal and connected to the fiber optic of the distributed fiber optic temperature measurement system to achieve temperature measurement of the joint conductor. Zhang Xiaoxin [17] designed an antenna using SAW surface acoustic wave temperature measurement technology for cable joint temperature measurement, which can transmit signals to the upper computer through the cable joint. Deng Zhifei [18] buried a passive wireless sensor inside the cable joint, transmitted energy to the temperature sensor through ultra-high-frequency electromagnetic waves, and obtained the temperature of the cable joint, which can be directly measured.

The thermal path modeling method and finite element simulation method are limited by the real-time nature of calculations and the diversity of cable structures, making it difficult to achieve real-time perception and measurement of cable joint hot spot temperature. The data mining method requires conducting temperature rise tests on cable joints, obtaining temperature data of measurement points and joint hot spots, and establishing a training sample set. Due to the limitations of temperature rise test conditions, it is difficult to fully consider the cable operating conditions in the training samples, which affects the universality of the model. The direct measurement method, as an implantable testing method, may pose potential hazards to the insulation of cables, and the service life of the testing equipment is often shorter than the service life of cable joints, making it difficult to achieve long-term testing. Meanwhile, current cable temperature measurement methods are limited to a single power quality. However, there may be a three-phase imbalance in the actual operation of power cable lines, leading to inconsistent losses in each phase of three-core cables [19], further affecting the universality of the aforementioned methods.

This article takes 10 kV three-core cable joints as the research object and constructs a three-dimensional finite element simulation model of 10 kV three-core cable joints. The feasibility of inverting the temperature of the joint hot spot through the surface temperature of the cable body was analyzed using the concept of "main heat flow". On this basis, based on the transient temperature field simulation of the three-core cable joint, a fitting relationship between the surface of the cable body and the hot spot temperature of the cable joint was established, achieving real-time sensing of the hot spot temperature of the three-core cable joint. Furthermore, considering the impact of three-phase load imbalance on the temperature field distribution of three-core cables, a fitting relationship for the hot spot temperature of three-core cable joints under three-phase load imbalance was constructed,

achieving real-time sensing of the hot spot temperature of three-core cable joints under three-phase load imbalance. This article further conducted multi-condition temperature rise tests on cable joints to verify the accuracy of the cable joint hot spot temperature inversion model.

2. Temperature Distribution Characteristics of Intermediate Joints in Three-Core Cables

2.1. Temperature Field Control Equation

In the calculation of the cable temperature field, the temperature field control equation can be divided into transient thermal analysis and steady-state thermal analysis, as shown in the following equation [20]:

$$\begin{cases} \frac{\partial^2 T}{\partial x^2} + \frac{\partial^2 T}{\partial y^2} + \frac{\partial^2 T}{\partial z^2} + \frac{\Phi}{\lambda} = 0 \\ \rho c \frac{\partial T}{\partial t} = \lambda \frac{\partial^2 T}{\partial x^2} + \lambda \frac{\partial^2 T}{\partial y^2} + \lambda \frac{\partial^2 T}{\partial z^2} + \Phi \end{cases} \tag{1}$$

In this formula, T is the temperature, in K units; C is the specific heat capacity of the material, in J/(kg·K); T is time, in seconds; ρ is the density of the material, in kg/m^3; λ is the thermal conductivity coefficient of the thermal conductive material, in W/(m·K); Φ is the heat generation, measured in W/m^3.

There are three types of boundaries related to heat transfer. The first type of boundary condition is a known boundary temperature function, which can be expressed as

$$T|_\Gamma = T_W \tag{2}$$

In this formula, Γ represents the outer boundary of the cable; T_W is the known temperature boundary, measured in K.

The second type of boundary condition is the known boundary normal heat flux density, expressed as

$$-\lambda \frac{\partial T}{\partial n}\bigg|_\Gamma = q \tag{3}$$

In this formula, q is the known heat flux density, measured in W/m^2.

The third type of boundary condition is the convective boundary condition, which refers to the known convective heat transfer coefficient and fluid temperature, expressed as

$$-\lambda \frac{\partial T}{\partial n}\bigg|_\Gamma = \alpha \left(T - T_f\right)\bigg|_\Gamma \tag{4}$$

In this formula, α is the convective heat transfer coefficient, measured in W/(m^2·K); T_f is the external fluid temperature, measured in K.

2.2. Temperature Field Calculation of Intermediate Joints in Three-Core Cables

(1) Calculation Model

The cable model studied in this article is 8.7/15 kV WLJ-3 × 300 mm^2. The cross-sectional structure of the cable body is shown in Figure 1. Its sequence from inside to outside is as follows: 1: cable core; 2: insulation layer (including inner and outer semi-conductive layers); 3: metal shielding layer; 4: fill layer; 5: inner sheath; 6: armor layer; 7: outer sheath.

The structure of the intermediate joint of the three-core cable is shown in Figure 2. The joints mainly include cable cores, compression joints, cold shrink prefabricated insulation components, copper mesh, and external related wrapping tapes. After the three-phase connectors with copper mesh are installed separately, they should be uniformly wrapped with waterproof tape and other materials outside the three-phase connectors. Due to the complex structure and lack of symmetry of the three-core cable joint, when establishing its model, it is divided into four parts: cable body, cable joint, cable joint and body connection,

and external armor (including internal air). Due to their irregular shape, the cable joints and the connecting parts of the body need to be separately established for each phase. The modeling of each part of the three-core cable joint is shown in Figure 3. The parameters of the cable body and joint materials are shown in Table 1.

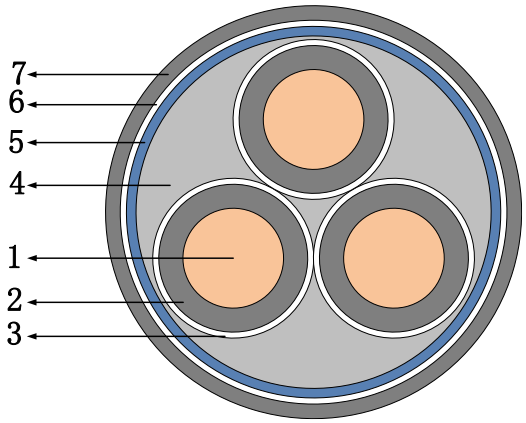

Figure 1. Three-core cable body cross-sectional structure diagram.

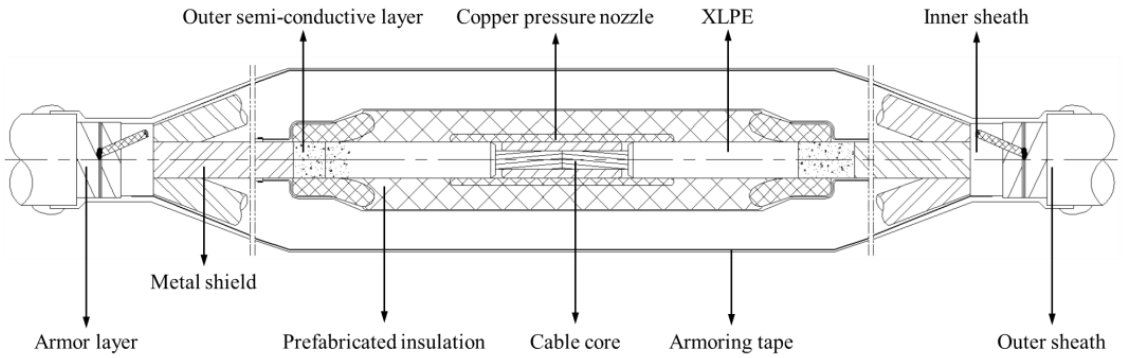

Figure 2. Three-core cable intermediate joint structure.

Table 1. Three-core cable joint material parameters [21–23].

Structure	Material	Thermal Conductivity/W/(m·K)	Density/kg/m^3
Cable core	Copper	383	8889
Pressure connecting pipe	Red copper	401	7830
Prefabricated insulation components	EPDM rubber	0.45	1100
Insulation layer	XLPE	0.286	920
Air	Air	0.023	1.293
PVC wrapping tape	Polyvinyl chloride	0.167	1450
Armoring tape	Fiberglass tape	0.036	2500

(2) Loading conditions

The heat source of the three-core cable joint consists of two parts. One part is the heating G_1 of the cable core, and the other part is the heating G_2 of the equivalent contact resistance at the joint crimping. It can be equivalently applied to a small area near the contact surface of the long- and short-end conductors of the joint, as shown in Figure 4.

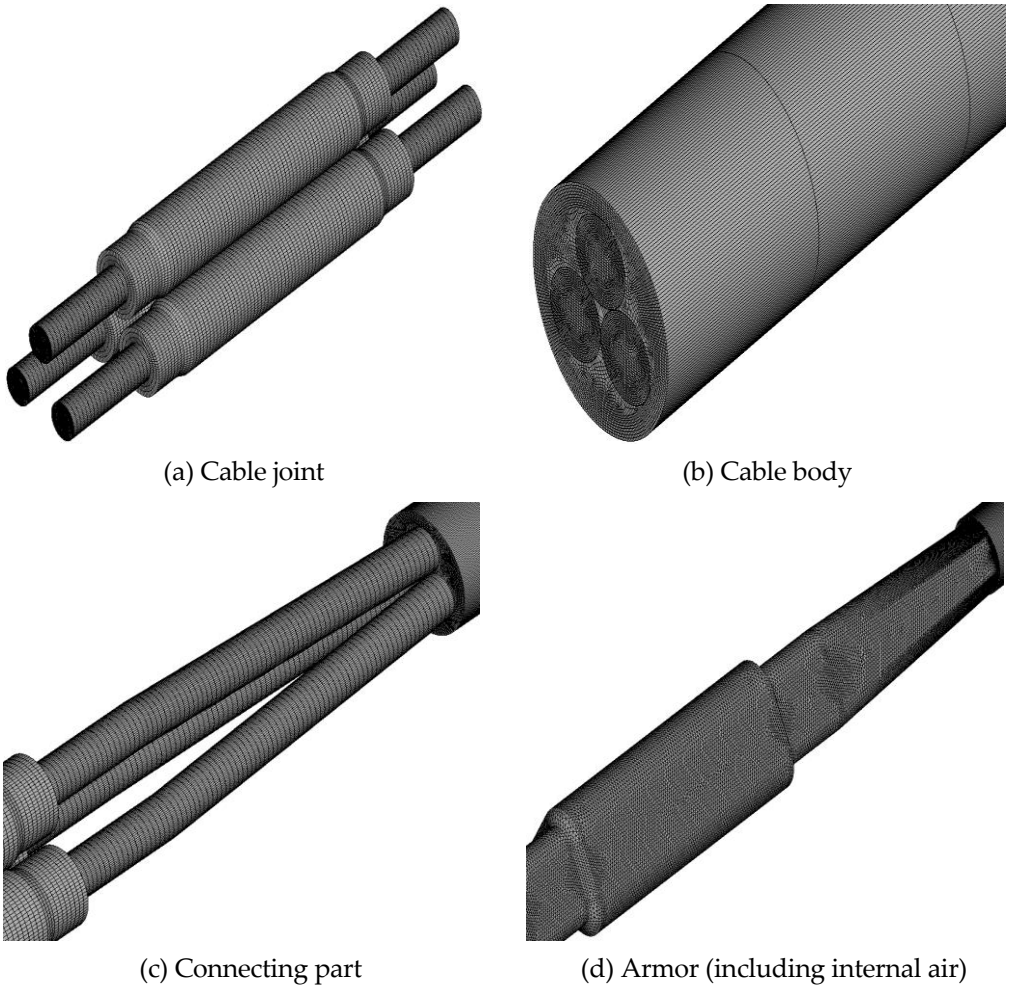

(a) Cable joint (b) Cable body

(c) Connecting part (d) Armor (including internal air)

Figure 3. Three-core cable joint and body simulation model.

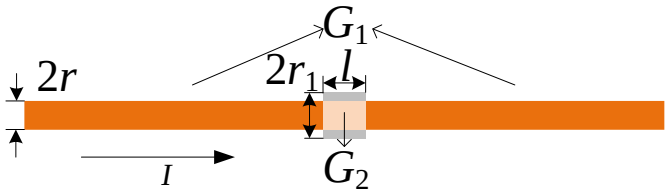

Figure 4. Cable core heat source loading diagram.

The two heat sources are calculated using the following formulas:

$$G_1 = \frac{I^2 R_1}{V} = I^2 \frac{\rho l_1}{S^2 l_1} = I^2 \frac{\rho}{\pi^2 r^4} \tag{5}$$

$$G_2 = \frac{W_2}{V} = \frac{I^2 R_2}{\pi r_1^2 l_2} \tag{6}$$

In these formulas, ρ is the resistivity of the copper conductor, in Ω·m; l_1 is the total length of the cable core, in meters; r_1 is the radius of the pressure connecting pipe, in meters; R_2 is the contact resistance of the joint, measured in Ω. After actual measurement during the production process, the contact resistances of the three phases were 7.05 μΩ, 7.47 μΩ, and 8.00 μΩ, respectively. It can be calculated that $G_1 = I^2 \times 0.17$ W/m^3, and the average of the contact resistances of the three phases is $G_2 = I^2 \times 0.301$ W/m^3.

The third type of temperature boundary condition, namely the convective heat transfer boundary condition, can be applied to the outer surface of the three-core cable joint. The convective heat transfer coefficient of the air is 8 W/(m^2·K), and the temperature of the surrounding air is 25 °C. The second type of temperature boundary condition can be loaded at the end of the body, which means that the normal heat flux density is zero, and temperature field simulation can be carried out when the cable core current is 500 A.

2.3. Temperature Distribution Characteristics of Intermediate Joints in Three-Core Cables

The simulation results are shown in Figure 5. It can be observed that the highest temperature point of the entire model is at the cable core inside the joint, while the lowest temperature point is at the armor tape on the surface of the joint. This is because the material applied outside the joint is thicker than the cable body and the thermal conductivity of the two materials is similar, making it difficult for the heat flow of the joint to transfer radially to the surface of the joint. The thermal resistance of the cable core is much smaller than that of other materials in the joint, and the heat flow of the joint easily flows axially towards the body on both sides, so the lowest temperature point is at the surface of the joint rather than the surface of the cable body. In addition, the temperature distribution of prefabricated insulation components is extremely uneven, with a temperature difference of 14 °C between the highest and lowest values. The temperature of the air and armor tape is higher at the contact point between the prefabricated component and the metal shielding layer, and lower at the distance. The reason is that there is more air distributed in non-contact areas, and the thermal conductivity of the air is extremely low, resulting in low temperatures in these areas. Similarly, the surface temperature of the cable body is also lower at positions far from the cable core and higher at positions close to the cable core. Due to the extremely irregular thermal conductivity and shape of the internal materials of cable joints, the temperature distribution inside the joints is extremely uneven.

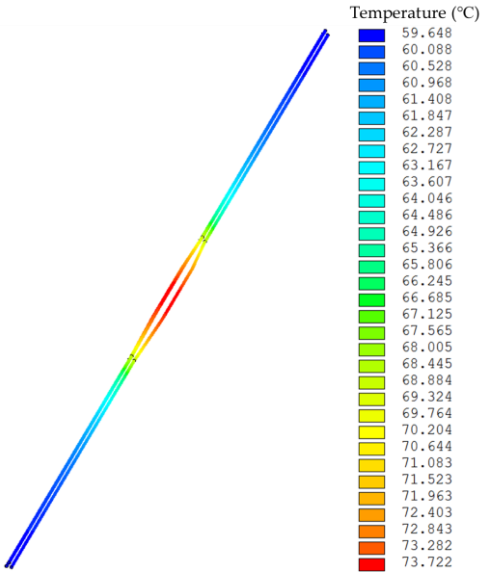

(a) Cable core

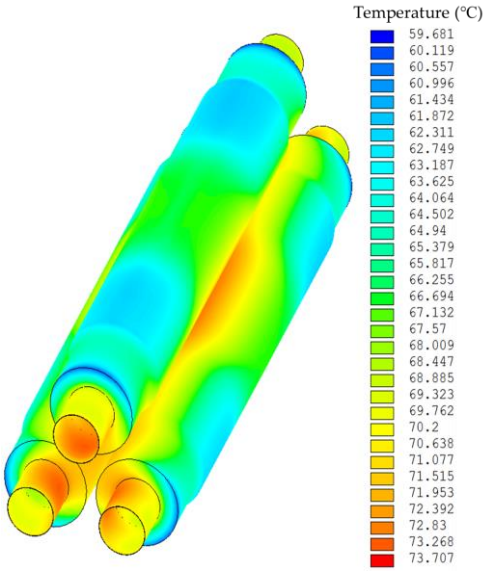

(b) Prefabricated silicone rubber

Figure 5. *Cont.*

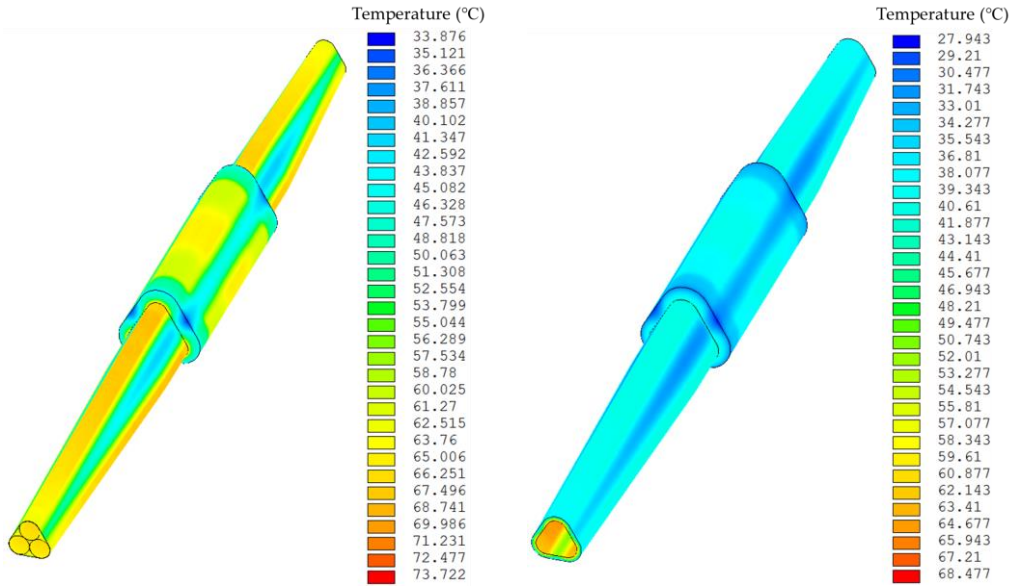

(c) Outsourced air (d) Armoring tape

Figure 5. Temperature field distribution of three-core cable joints.

3. Inversion of Hot Spot Temperature at the Intermediate Joint of Three-Core Cable

3.1. Inversion Ideas for Intermediate Joint Temperature

For a temperature field containing a heat source, the heat source emits heat outward in the form of heat flux. The difference between the heat absorption and dissipation of any microelement in the field causes the temperature rise of the object, which in turn constitutes the temperature distribution of the entire field. It can be said that heat flux is the direct driving force for the formation of a temperature field, and also the link connecting the temperatures at various points within the field [24]. Obviously, when there is no heat flow path connection between two points, a change in temperature at one point will not cause a change in temperature at the other point, meaning that there is no correlation between the temperatures of the two points. On the contrary, the larger the heat flux on the path, the stronger the temperature correlation between each point on the path, and the path with the highest heat flux can be called the "main heat flux". Based on the above analysis, in order to ensure a strong correlation between the temperature of feature points and the temperature of hot spots, the selection of inversion paths should be based on the principle of maximizing heat flux, and the inversion feature points should be placed on the main heat flux path as much as possible [25].

For the intermediate joint of a three-core cable, the heat source is the current-carrying conductor, and the heat flow transmitted can be simplified into two directions: radial and axial. According to the analysis in Section 2.3, due to the thick material applied outside the joint and the low thermal conductivity, the heat flow at the joint is not easily transmitted to the surface of the joint in the radial direction. On the contrary, due to the much greater thermal conductivity of the conductor than the surrounding insulation, the direction of the axial main heat flux of the three-core cable joint is the axial direction of the current-carrying conductor. In practical applications, the temperature on the current-carrying conductor of the cable cannot be directly measured, while the measurement of the surface temperature of the cable is relatively simple, considering that the insulation material thickness in the radial direction of the cable body is smaller compared to the thickness at the joint. Based on the concept of "main heat flow", the characteristic points for temperature inversion of the hot spot of the three-core cable joint should be located on the surface of the cable body, as shown in Figure 6.

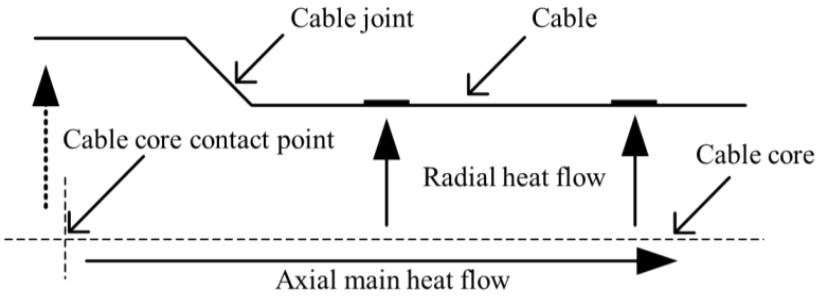

Figure 6. Heat flow distribution in three-core cable joint.

3.2. Inversion of Joint Hot Spot Temperature Based on Temperature Fitting

(1) Inversion function fitting

Based on the simulation results of the temperature field, the fitting of cable joint hot spot temperature is carried out, which involves obtaining several datasets of cable body surface temperature and joint hot spot temperature through temperature field simulation. The function fitting method is used to establish the relationship between the surface characteristic point temperature of the cable body and the joint hot spot temperature. x = 0.775, x = 1.775, and x = 2.875 were initially selected as inversion feature points, with their temperatures represented by T_1, T_2, and T_3, respectively. The temperature of the cable joint core at x = 0 is represented by T0, and the schematic diagram of the axial inversion point position is shown in Figure 7.

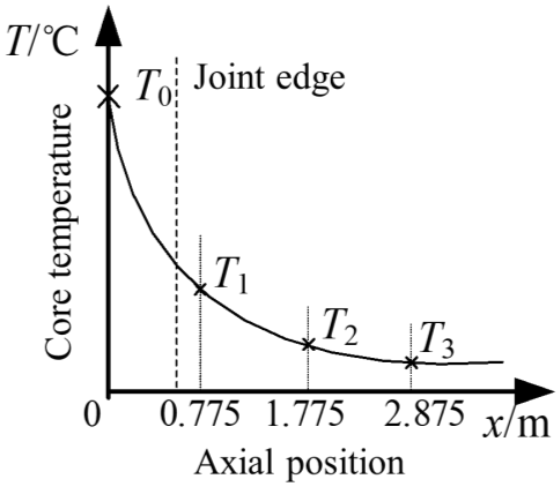

Figure 7. Schematic diagram of inversion feature point locations.

This article conducts a single-step transient temperature field simulation with a loading current of 100 A to 600 A at intervals of 100 A and conducts a total of six transient calculations. The initial temperature and ambient temperature for each calculation are 25 °C, the convective heat transfer coefficient is 8 W/(m^2·K), and the calculation time for each single step is 20 h. A set of transient result data is taken every 20 min, including the inversion points of three main cable cores and the hot spot temperatures of each phase of the three-core cable cores.

The purpose of temperature inversion is to find the mathematical relationship between the surface temperature of the cable body and the hot spot temperature of the cable joint, with the former being the independent variable and the latter being the dependent variable. This article uses a power exponential polynomial for fitting, where the number of feature

points n is 3 and the highest power m is 2. Therefore, the temperature T_0 of the cable joint core can be expressed as

$$\begin{aligned} T_0 &= f(T_1, T_2, T_3) \\ &\approx f_1(T_1) + f_2(T_2) + f_3(T_3) \\ &\approx a_1 \cdot T_1^2 + b_1 \cdot T_2^2 + c_1 \cdot T_3^2 \\ &+ a_2 \cdot T_1^1 + b_2 \cdot T_2^1 + c_2 \cdot T_3^1 + e \end{aligned} \tag{7}$$

Here, T_1, T_2, and T_3 represent the temperatures at the inversion points on the surface of the three cable bodies, respectively, and a_i, b_i, c_i, and e are the coefficients of each temperature-independent variable in the polynomial. $f(T_1, T_2, T_3)$ is the true function expression between the three temperature inversion points and the joint hot spot temperature.

Based on the transient temperature dataset obtained from the simulation, the parameters of the above function expression were fitted using Levenberg Marquardt and the universal global optimization method. The coefficients of the function expression can be obtained as shown in Table 2. The fitted mean square error (RMSE) is 0.1199, and the correlation coefficient (R) is 0.99998, indicating a good agreement between the fitted value and the original value.

Table 2. Coefficients of joint hot spot temperature fitting expression.

Coefficient	Numerical Value	Coefficient	Numerical Value
a_1	−0.0347	a_2	10.0049
b_1	0.2039	b_2	−40.1406
c_1	−0.1655	c_2	30.6402
e	10.1277		

(2) Inversion verification of joint hot spot temperature

To verify the accuracy of axial temperature inversion, a transient simulation of a multi-step current was conducted. The multi-step current is 500 A-400 A-300 A-600 A-200 A-100 A-300 A-400 A-550 A-500 A, and each current segment remains unchanged for 2 h. The duration of each cycle is 20 h. Two cycles need to be calculated, and the same boundary conditions need to be applied for a total duration of 40 h. By calculating the transient temperature field, datasets related to T_0, T_1, T_2, and T_3 can be obtained. By substituting T_1, T_2, and T_3 into the temperature inversion function, the corresponding fitted temperature dataset T_0' can be obtained. Comparing T_0' and T_0, as shown in Figure 8, it can be observed that there is a significant temperature difference at the point of current mutation. Over time, the temperature difference gradually stabilizes, with a stable error within 3 °C.

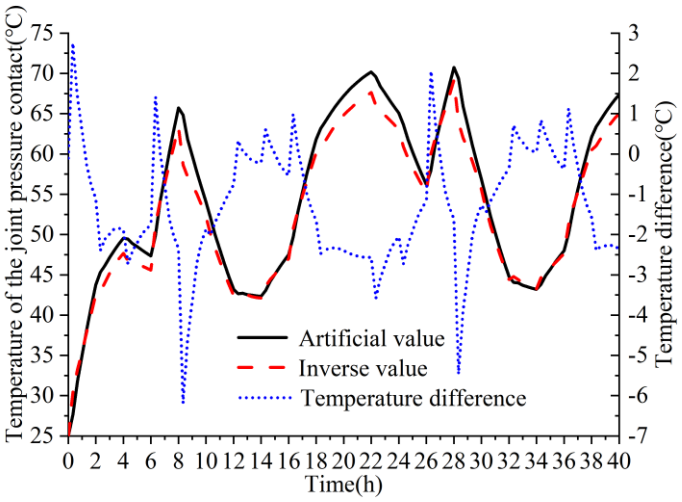

Figure 8. Comparison of inversion results and simulation results.

4. Inversion of Joint Hot Spot Temperature Due to Three-Phase Load Imbalance

The premise for the inversion of cable joint hot spot temperature mentioned earlier is the three-phase load balance of the three-core cable, and the selection of samples in the process of establishing the joint hot spot temperature fitting function is also based on the three-phase load balance of the three-core cable. In practical situations, three-phase loads often have imbalances [19], and the feasibility of using this fitting function still remains to be explored in cases of three-phase load imbalance. The following will analyze the fitting effect of the inversion function when the three-phase load of the three-core cable is unbalanced.

This article defines three-phase imbalance as the ratio of the difference between the maximum and minimum load currents and the maximum value [26]. The calculation formula for its imbalance degree β is Equation (8), where I_{max} and I_{min} are the maximum and minimum values of the three-phase current, respectively, in units of A. For example, if the three-phase currents are 500 A, 450 A, and 400 A respectively, the imbalance degree is 20%. In the simulation, the average of the maximum and minimum values is taken as the intermediate value of the current.

$$\beta = \frac{I_{max} - I_{min}}{I_{max}} \times 100\% \quad (8)$$

4.1. The Impact of Three-Phase Load Imbalance on the Inversion of Joint Hot Spot Temperature

According to the analysis of the main heat flux of cable joints, under the condition of unbalanced three-phase load, the current magnitude of three-phase conductors is not equal, and the heat generation is also not equal. However, due to the fact that the thermal conductivity of the conductor is much greater than that of the surrounding insulation, in the case of unbalanced three-phase loads, the direction of the axial main heat flow of the three-core cable joint is still the axial direction of the current-carrying conductor.

(1) Radial temperature distribution of the body under unbalanced three-phase load

In the previous analysis, the inversion feature points were located on the surface of the cable body, and further exploration is needed to investigate the impact of three-phase load imbalance on the mapping relationship between surface temperature and cable core temperature. The current levels of phases A, B, and C under different unbalanced three-phase load conditions are shown in Table 3. A temperature field simulation was conducted at an ambient temperature of 25 °C and a surface convective heat transfer coefficient of 8 W/(m^2·K). The simulation results are shown in Figure 9. It can be seen that under different unbalanced three-phase load conditions, there are significant differences in the radial temperature distribution of the three-core cable body.

Table 3. Different three-phase load unbalanced simulation conditions.

Unbalance Factor	A-Phase Current/A	B-Phase Current/A	C-Phase Current/A
Unbalance 10%	500	475	450
Unbalance 50%	500	375	250
Two-phase Unbalance 50%	500	250	250
Single-phase Unbalance 50%	500	500	250

(2) Exploration of mapping relationships based on thermal path models

In order to further explore the impact of three-phase load imbalance on the mapping relationship between surface temperature and cable core temperature, this article constructs a radial transient thermal circuit model of the three-core cable body based on the structural and material parameters of the three-core cable body, as shown in Figure 10.

In Figure 10, P_c and P_d represent the conductor loss and insulation medium loss of the cable core, respectively; λ_1 and λ_2 are the loss factors of the metal shielding layer and the armor layer, respectively; T_1, T_2, and T_3 represent the temperature of the cable core

layer, the temperature of the metal shielding layer, and the temperature of the armor layer, respectively; T_0 is the temperature of the outer sheath, equivalent to a thermal pressure source; R_2, R_4, and R_6 represent the thermal resistance of the insulation layer, filling layer, inner sheath, and outer sheath; C_1~C_6 represent the heat capacity of conductors, the heat capacity of the insulation layer, the equivalent heat capacity of the metal shielding layer, the heat capacity of the filling layer and inner sheath, and the heat capacity of armor layer and outer sheath.

The three-phase load current changes of A, B, and C can be set as shown in Figure 11, with each current segment lasting for 4 h and a total duration of 40 h. A temperature field simulation can be conducted at an ambient temperature of 25 °C and a surface convective heat transfer coefficient of 8 W/(m^2·K). The surface temperature of the cable outer sheath obtained from the simulation can be substituted into the thermal circuit model, and the temperature of the cable core can be calculated and compared with the finite element calculation results. The comparison results are shown in Figure 12. The temperature difference between the temperature calculation results of the thermal path model cable core and the finite element cable core temperature calculation results is shown in Figure 12b. It can be observed that when the three-phase current is unbalanced, the surface temperature of the cable body can still be accurately calculated for the cable core temperature at each corresponding position. Therefore, in the case of unbalanced three-phase loads, the mapping relationship can still be used to fit the hot spot temperature of cable joints.

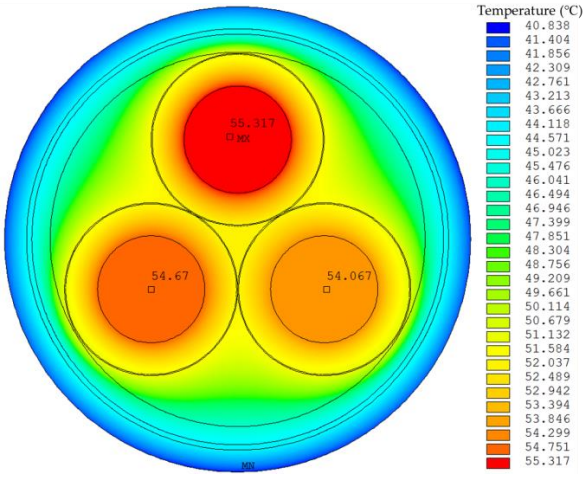

(a) Unbalance 10%

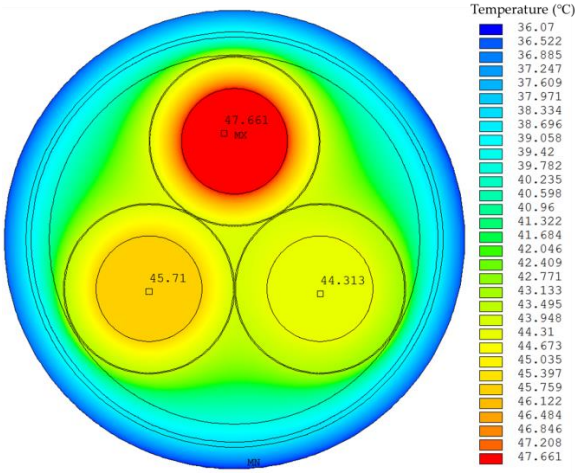

(b) Unbalance 50%

Figure 9. *Cont.*

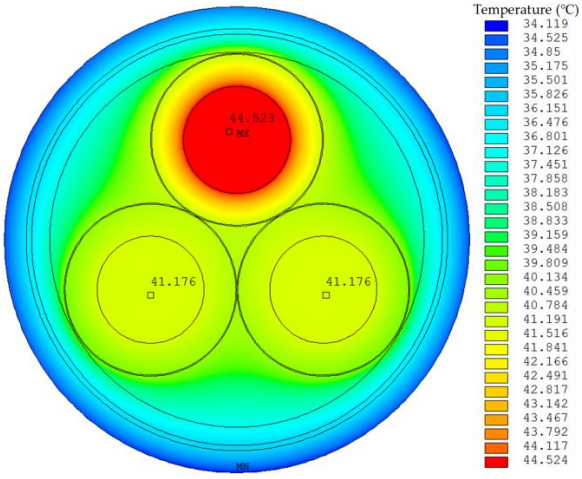

(c) Two-phase Unbalance 50%

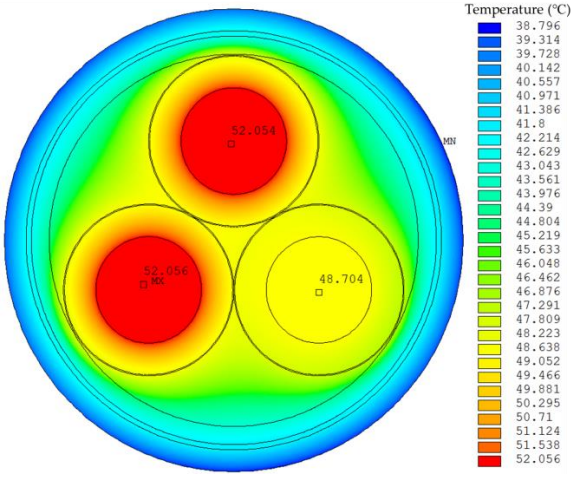

(d) Single-phase Unbalance 50%

Figure 9. Radial temperature distribution of cable body under different unbalanced conditions.

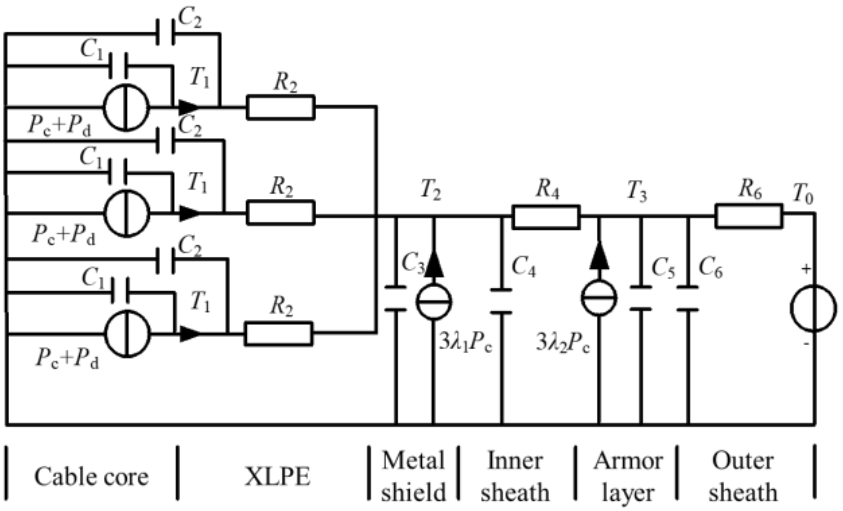

Figure 10. Radial transient thermal path model of three-core cable body.

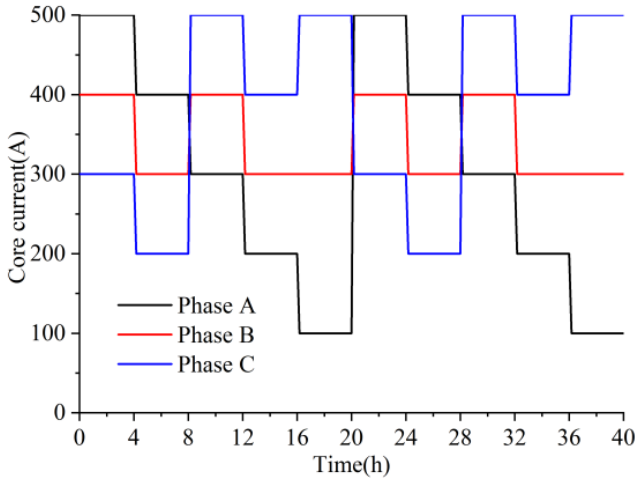

Figure 11. Three-core cable core current.

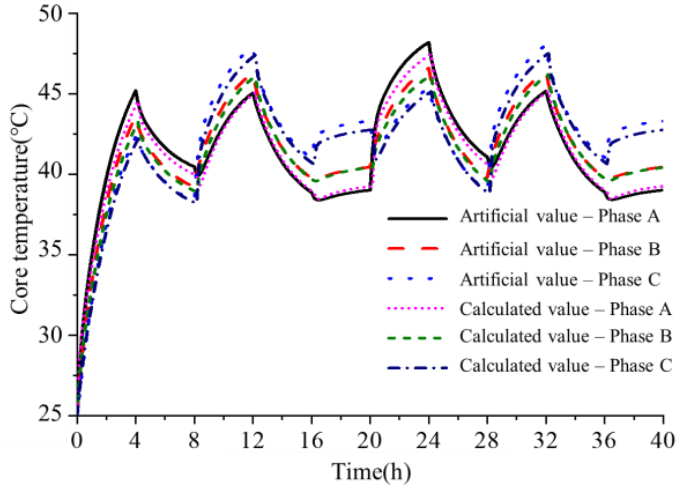

(a) Temperature rise curve of three-core cable core

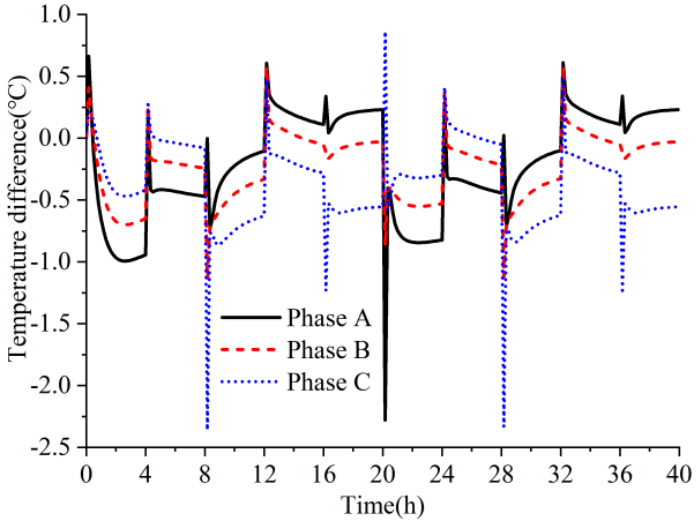

(b) Temperature difference curve of three-core cable core

Figure 12. Three-core cable transient thermal path model calculation results.

4.2. Inversion of Joint Hot Spot Temperature under Three-Phase Load Imbalance

(1) Inversion of fitting formulas under load-balancing conditions

Based on the above analysis, the inversion function obtained by fitting under load balance conditions is used to invert the temperature of the joint hot spot. The inversion results are shown in Figure 13. It can be seen that the overall inversion error is relatively large, with a maximum error close to 5 °C. Therefore, it is not possible to directly use the joint hot spot inversion formula obtained under load-balancing conditions to fit the joint hot spot temperature under three-phase load imbalance.

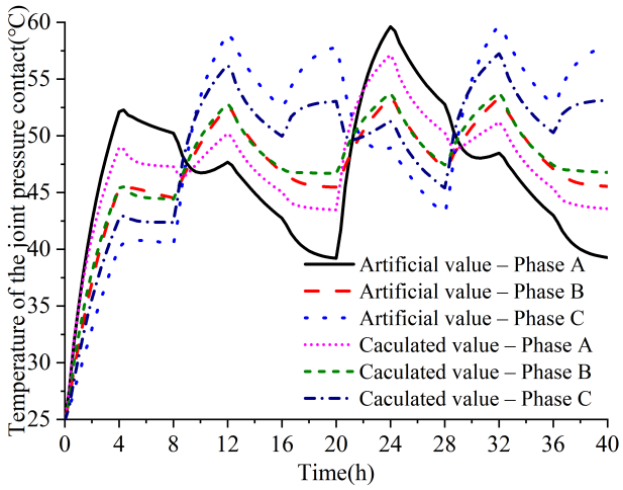

(a) Hot spot temperature rise curve of three-core cable

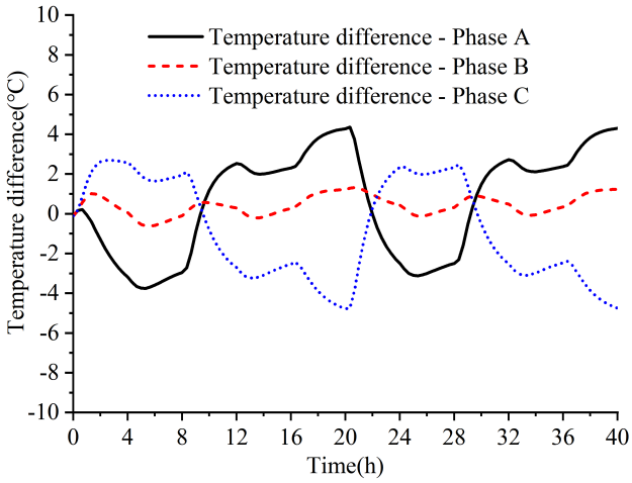

(b) Three-core cable hot spot temperature difference curve

Figure 13. Three-core cable joint hot spot temperature inversion results (load balance fitting formula).

(2) Inversion of joint hot spot temperature under three-phase load imbalance

In order to obtain the inverse fitting function of the joint hot spot temperature of the three-core cable under a three-phase load imbalance, the temperature field of the three-core cable joint under different currents and balance degrees was calculated, and its transient temperature data were extracted for fitting. The selected imbalance degree and maximum current are shown in Table 4. Eighty-one sets of simulation data were obtained by taking the maximum, minimum, and average intermediate currents for each balance degree. The initial temperature and ambient temperature for each calculation are 25 °C, the convective heat transfer coefficient is 8 W/(m^2 ·K), and the calculation time for each single step is 18 h with an interval of 20 min.

Table 4. Unbalance parameter selection.

Unbalance Factor/%	Maximum Current Value/A
10	100
30	300
50	500

Eighty-one sets of transient temperature rise data simulated under three-phase load imbalance of the three-core cable joint and six sets of transient temperature rise data under load balance can be fitted according to Formula (7). The coefficients of the fitting expressions for the temperature T_0 at the joint crimping point and the corresponding cable core temperature (T_1, T_2, T_3) at the body temperature measurement point are shown in Table 5. The fitted mean square error (RMSE) is 0.2267, and the correlation coefficient (R) is 0.99988, indicating a good agreement between the fitted value and the original value.

Table 5. Coefficients of joint hot spot temperature fitting expression considering three-phase load unbalance.

Coefficient	Numerical Value	Coefficient	Numerical Value
a_1	0.0013	a_2	9.3365
b_1	0.0395	b_2	−41.7454
c_1	−0.0424	c_2	33.1777
e	6.7845		

4.3. Inversion Verification of Joint Hot Spot Temperature under Three-Phase Load Imbalance

To verify the accuracy of the fitting function for joint hot spot temperature inversion, a transient simulation of multi-step currents was conducted, with each current segment kept constant for 4 h and a total duration of 40 h. By calculating the transient temperature field, datasets related to T_0, T_1, T_2, and T_3 can be obtained. By substituting T_1, T_2, and T_3 into the temperature inversion function, the corresponding fitted temperature dataset T_0' can be obtained. T_0' and T_0 can be compared, as shown in Figure 14. From the graph, it can be observed that the temperature difference increases at the point of sudden current changes, and over time, the temperature difference gradually stabilizes with a stable error of within 1.5 °C.

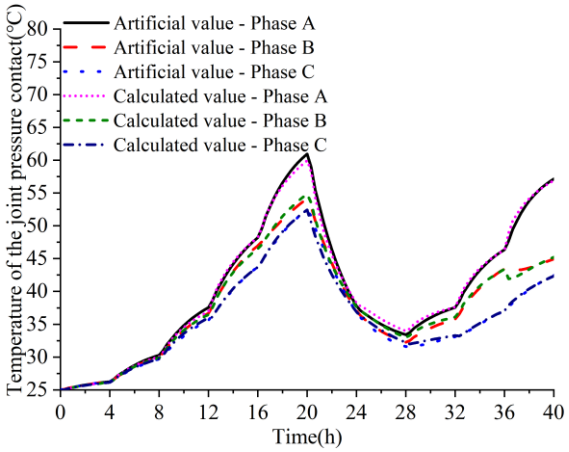

(a) Hot spot temperature rise curve of three-core cable

Figure 14. *Cont.*

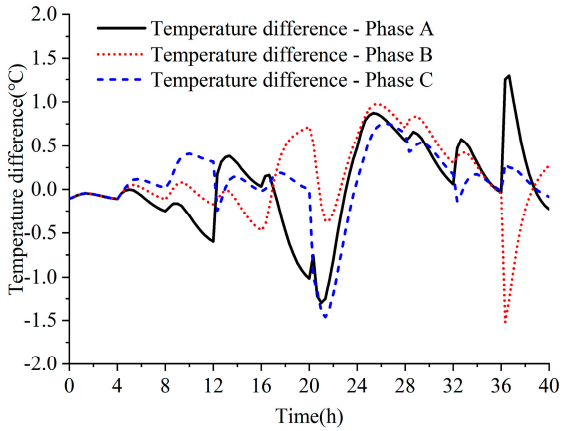

(b) Temperature difference curve of three-core cable joint hot spot

Figure 14. Three-core cable joint hot spot temperature inversion results (load unbalance fitting formula).

5. Temperature Rise Test Verification

At present, the inversion method for joint hot spot temperature of three-core cables under an unbalanced three-phase load based on temperature measurement on the outer surface of the cable has been verified through finite element simulation results, but its inversion effect in actual cable joints still needs to be verified. To this end, a test circuit for three-core cable joints was constructed, and high-precision temperature sensors were installed inside the cable joints and on the cable surface. By loading short-term continuous and long-term fluctuating load currents in the cable circuit, the actual effect of the entire cable joint temperature inversion algorithm was experimentally verified by comparing the measured and inverted temperatures of the cable joints.

5.1. Inversion Verification of Joint Hot Spot Temperature under Three-Phase Load Imbalance

The temperature rise test platform for three-core cable joints mainly consists of five parts, and its overall layout is shown in Figure 15:

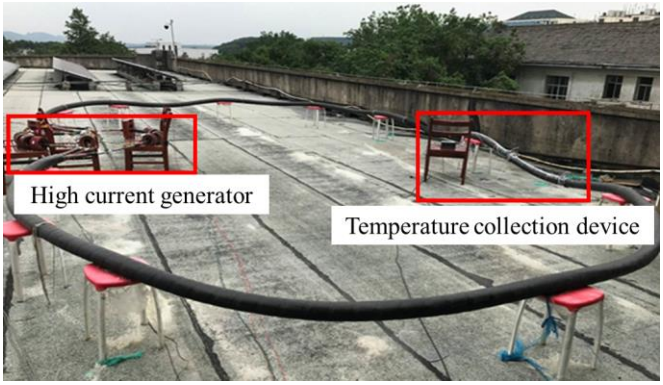

Figure 15. Three-core cable joint temperature rise test circuit.

(1) Cable joint test circuit: The circuit consists of the cable body and joints, with a total length of 24 m. The cable model is YJV22-8.7/15 kV-3 × 300 mm^2 (cross-linked polyethylene-insulated steel-tape-armored polyvinyl chloride-sheathed power cable), and the nominal cross-sectional area of the cable core is 300 mm^2.

(2) High-current generator: A high-current generator consists of an autotransformer and a current-boosting coil, which adjusts the current of the test circuit by adjusting the output voltage of the autotransformer.

(3) Temperature and current acquisition device: A temperature and current acquisition device consists of a temperature sensor, current transformer, temperature acquisition card, current acquisition card, and upper computer, used to monitor and record the current of the test circuit and the temperature of the temperature monitoring points in real time during the test process.

(4) Support fixing device: A cable test circuit support device consists of multiple stools with a certain load-bearing capacity.

(5) Sunshade net: It can prevent the influence of solar radiation on joint temperature inversion.

To change the imbalance of the load current, the number of current-boosting coils per phase can be changed. Taking a certain phase's rising current coil as an example, it can be assumed that the phase has three rising current coils, which are connected in parallel to the secondary side of the autotransformer. By changing the on/off of the switch, the number of current raising coils connected to the circuit can be changed, as shown in Figure 16. S1 can be disconnected first, and then S4 can be closed, which can disconnect the coil from the circuit and short-circuit itself. In order to study the inversion effect under different load imbalances, the selected coil combinations and experimental loading conditions are shown in Table 6.

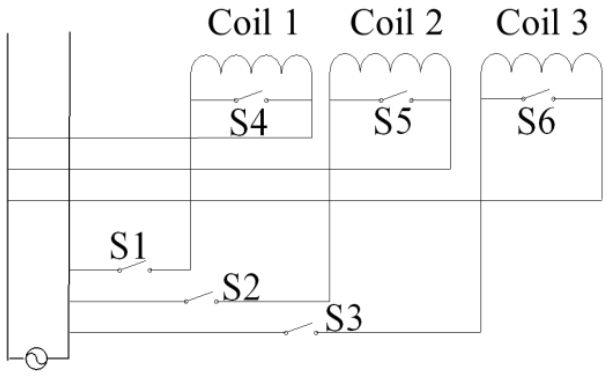

(a) Schematic diagram

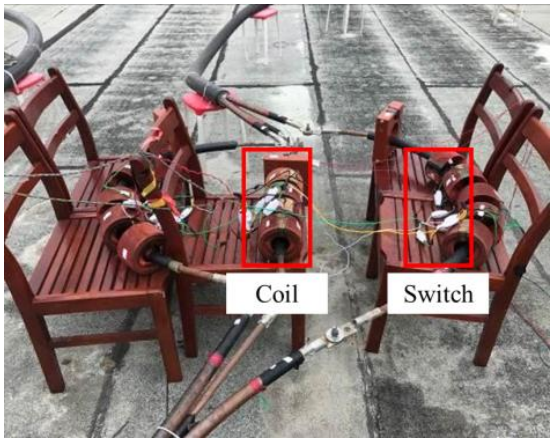

(b) Physical image

Figure 16. Upstream coil wiring diagram.

Table 6. Unbalance and test duration for different coil combinations.

Number	Number of Coils			Unbalance Factor/%	Duration/h
	A-Phase	B-Phase	C-Phase		
1	3	4	3	4.9	8
2	5	2	5	49.9	3
3	5	2	1	49.4	3
4	4	2	1	43.7	8
5	3	4	1	40.7	3
6	5	4	4	27.2	3
7	4	4	4	20.6	3
8	2	4	3	14.7	3
9	5	1	5	60.8	3

5.2. Verification of Joint Hot Spot Temperature Inversion Test

The experiment lasted for a total of 48 h, and the changes in three-phase load current during the experiment are shown in Figure 17. The inversion results of the joint hot spot temperature obtained using the proposed cable joint hot spot temperature inversion method are shown in Figure 18. When the current is in a changing state, since the change in the temperature measurement point on the cable surface lags behind the change in the hot spot temperature inside the joint, the error in the hot spot temperature of the joint obtained by fitting is large. The vast majority of these errors are within 3 °C, with a maximum error not exceeding 4.5 °C, meeting the engineering error requirements.

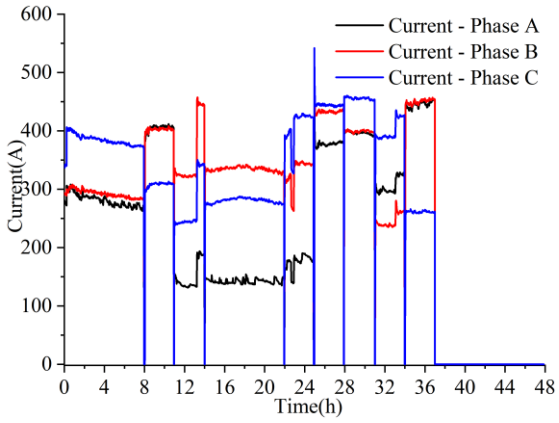

Figure 17. Temperature rise test current curve.

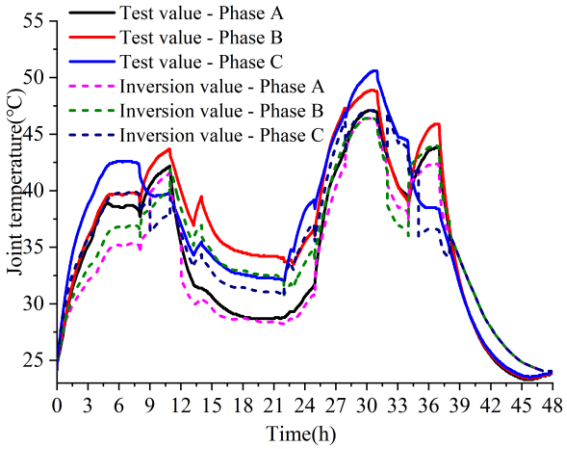

(a) Temperature rise curve

Figure 18. *Cont.*

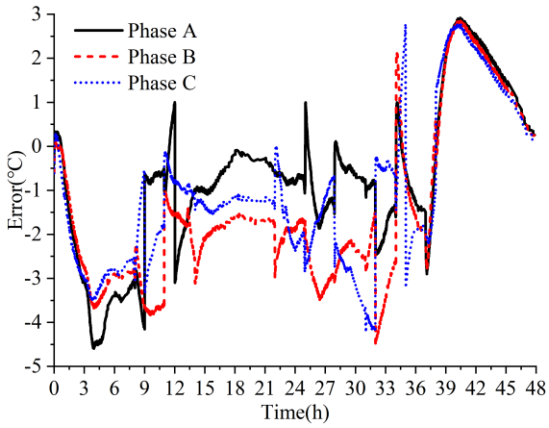

(b) Error curve

Figure 18. Three-core cable joint temperature inversion results.

6. Conclusions

Temperature is a key factor affecting the insulation performance and operational safety of cable joints. Accurately obtaining the hot spot temperature of cable joints is a difficult problem in cable operation and maintenance. Three-core cables may have unbalanced three-phase loads during actual operation. This article is guided by the problem of inverse perception of joint hot spot temperature under three-phase load imbalance in three-core cables. Based on the idea of "main heat flow" in cable intermediate joints, a three-core cable intermediate joint hot spot temperature inversion model considering three-phase load imbalance is established. The main conclusions are as follows:

(1) A three-dimensional finite element simulation model of 10 kV three-core cable joints was constructed, and the feasibility of inverting the joint hot spot temperature through the surface temperature of the cable body was analyzed using the concept of "main heat flow". On this basis, based on the transient temperature field simulation of the three-core cable joint, a fitting relationship between the surface of the cable body and the hot spot temperature of the cable joint was established, achieving real-time sensing of the hot spot temperature of the three-core cable joint.

(2) This article analyzes the differences in the radial temperature distribution of the cable body under three-phase load imbalance in three-core cables and verifies the effective mapping relationship between the surface temperature of the cable body and the temperature of the joint hot spot under three-phase load imbalance in combination with the radial transient thermal circuit model of the three-core cable body. Further construction of a three-core cable joint hot spot temperature inversion model suitable for three-phase load imbalance has been carried out, achieving the real-time perception of joint hot spot temperature in this special case.

(3) A multi-step three-phase unbalanced load temperature rise test was conducted on the three-core cable joint, and the accuracy of the hot spot temperature inversion model of the three-core cable joint was verified. The maximum error of the transient inversion of the hot spot temperature did not exceed 4.5 °C, and the steady-state error was basically within 3 °C, achieving high inversion accuracy.

Author Contributions: Conceptualization, X.L.; methodology, Z.Z. and J.R.; software, T.Y.; validation, B.N.; writing—original draft preparation, X.L., Z.Z., T.Y., J.R. and B.N. All authors have read and agreed to the published version of the manuscript.

Funding: This research was funded by the National Natural Science Foundation of China (No. U2066217) and the Science and Technology Project of China Southern Power Grid Company Limited (No. GDKJXM20220135).

Data Availability Statement: The data presented in this study are available on request from the corresponding author.

Conflicts of Interest: Authors Xinhai Li, Zhifang Zhang, and Ting Yang are employed by the company Guangdong Zhongshan Power Supply Bureau of China Southern Power Grid Co., Ltd. The remaining authors declare that the research was conducted in the absence of any commercial or financial relationships that could be construed as a potential conflict of interest. The authors declare that this study received funding from China Southern Power Grid Company Limited. The funder was not involved in the study design, collection, analysis, interpretation of data, the writing of this article or the decision to submit it for publication.

References

1. The National Development and Reform Commission. *Guiding Opinions on Accelerating the Construction and Renovation of Distribution Networks*; National Development and Reform Commission: Beijing, China, 2015.
2. National Energy Administration. *Notice on the Action Plan for Construction and Renovation of Distribution Networks (2015–2020)*; National Energy Administration: Beijing, China, 2015.
3. Gao, Z. *Research on Online Current Carrying Capacity Prediction System for Power Cables*; Harbin Institute of Technology: Harbin, China, 2005.
4. Liu, G.; Lei, C.; Liu, Y. Analysis on transient error of simplified thermal circuit model for calculating conductor temperature by cable surface temperature. *Power Syst. Technol.* **2011**, *35*, 212–217.
5. Yang, L.; Li, Z.; Hao, Y.; Fu, M. Calculation of current-carrying capacity of HVDC cable joint under constraints of operating temperature and temperature difference of insulating layer. *Autom. Electr. Power Syst.* **2016**, *40*, 129–134.
6. Huang, J.; Fan, D.; Liang, Y.; Zhu, Z.; Liu, W. Analysis of the influencing factors of the cable thermal path model and its optimization method. In Proceedings of the 2023 8th Asia Conference on Power and Electrical Engineering (ACPEE), Tianjin, China, 14–16 April 2023; pp. 2554–2560.
7. Jiang, H.; Zhao, X.; Liang, Y.; Fu, C. Temperature Rise and Ampacity Analysis of Buried Power Cable Cores Based on Electric-magnetic-thermal-moisture Transfer Coupling Calculation. In Proceedings of the 2023 13th International Conference on Power and Energy Systems (ICPES), Chengdu, China, 15–17 December 2023; pp. 261–265.
8. Bian, X.; Chen, Y.; Zhou, Q.; Zhang, Y.; Wei, B.; Tong, P. Dynamic Temperature Field Calculation and Short-time Allowable Ampacity Evaluation of Submarine Cable Based on Thermal Analytical Model. *High Volt. Eng.* **2023**, *49*, 793–802.
9. Liang, Y.; Wang, J. Transient Temperature Rise Calculation of Buried Power Cable Based on Thermal Circuit Model and Transient Adjoint Model. *High Volt. Eng.* **2022**, *48*, 3517–3525.
10. Yang, F.; Cheng, P.; Luo, H.; Yang, Y.; Liu, H.; Kang, K. 3-D thermal analysis and contact resistance evaluation of power cable joint. *Appl. Therm. Eng.* **2016**, *93*, 1183–1192. [CrossRef]
11. Fu, J.; Cheng, P.; Chen, W.; Hu, X.; Wang, Q.; Yang, Q.; Yang, F. Investigation of the effects of insulation defects on the 3-D electromagnetic-thermal coupling fields of power cable joint. In Proceedings of the IEEE Conference on Industrial Electronics and Applications, Hefei, China, 5–7 June 2016.
12. Zhang, X.; Fu, X.; Li, J.; Ji, L.; Luo, J. Simulation Analysis of 10kV Cable Joint Based on Electromagnetic and Thermal Field Coupling. *Electr. Eng.* **2022**, *21*, 1–4.
13. Xiao, W.; Han, Q.; Zhu, W. Temperature prediction of cable joints based on generalized regression neural network. *Electr. Power* **2013**, *32*, 34–37.
14. Wu, T.; Zhu, H.; Zhan, Q. Indirect Measurement Method of Cable Joint Core Temperature Based on BP Neural Network Optimized by Improved SSA. *Sci. Technol. Eng.* **2023**, *23*, 9048–9055.
15. Yuan, Y.; Gao, L.; Zhu, C.; Ye, Z.; Zou, H. Temperature measurement and calculation method for high voltage three-core cable joint based on support vector regression. *Distrib. Util.* **2023**, *40*, 85–91.
16. Lv, G.; Zhang, D.; Fu, C.; Yang, N.; Zhou, C.; Wu, X.; Liu, B. Split Conductor in Preset Temperature Fiber XLPE Cables and Accessories of the Development and Test. *Electr. Wire Cable* **2013**, 8–11.
17. Zhang, X.; Zhang, X.; Lin, F. Research on Internal Temperature Mearsuring Antenna in Cable Jionts Based on SAW. *Piezoelectr. Acoustpppptics* **2023**, *45*, 178–182.
18. Deng, Z.; Bao, G. Online Monitoring System of Cable Joint Temperature Based on UHF RFID Technology. *Instrum. Tech. Sens.* **2021**, 71–75+96.
19. Chen, Z.; Wu, Z.; Liu, H.; Chen, D. Influence of Voltage Deviation and Three-phase Unbalance on Clble Line Loss. *Guangdong Electr. Power* **2020**, *33*, 125–132.
20. Yang, Y.; Wang, Q.; Liu, Z. Simulation of Underground Cable Temperature Distribution Based on Multiphysics Modeling. In Proceedings of the 2021 11th International Conference on Power, Energy and Electrical Engineering (CPEEE), Shiga, Japan, 26–28 February 2021; pp. 26–31.
21. Dong, Y.; Li, Z.; Wang, H.; Du, B.; Tang, Q.; Meng, Z. Characteristics of Temperature Distribution and Current Carrying Capacity of XLPE Cable Joint. In Proceedings of the 2023 IEEE 4th International Conference on Electrical Materials and Power Equipment (ICEMPE), Shanghai, China, 7–10 May 2023; pp. 1–4.
22. Liu, G.; Wang, P.; Mao, J.; Liu, L.F.; Liu, Y.G. Simulation Calculation of Temperature Field Distribution in High Voltage Cable Joints. *High Volt. Eng.* **2018**, *44*, 3688–3698.

23. Qiin, C.; Li, B.; Li, G.; Yang, X.; Lin, C. Numerical Calculation of Temperature Field of 220kV Three—Core Submarine Cable Based on Finite Element Method. *J. Northeast Electr. Power Univ.* **2019**, *39*, 5–10.
24. Tang, L.; Ruan, J.; Yang, Z.; Chen, R.; Li, G.; Yin, X. Hotspot Temperature Monitoring of Fully Insulated Busbar Taped Joint. *IEEE Access* **2019**, *7*, 66463–66475. [CrossRef]
25. Quan, Y.; Ruan, J.; Gong, R.; Chen, J.; Jin, X.; Wen, W. Transformer hot-spot temperature inversion method based on streamline and support vector regression. *Adv. Technol. Electr. Eng. Energy* **2018**, *37*, 23–31.
26. *SD 292-1988*; Operating Regulations for Overhead Distribution Lines and Equipment. National Development and Reform Commission: Beijing, China, 1988.